Simulated Sea Surface Salinity variability in the tropical Pacific

Xiaochun Wang and Yi Chao

Jet Propulsion Laboratory, California Institute of Technology, Pasadena, California, USA

Received 7 October 2003; accepted 19 December 2003; published 21 January 2004.

[1] Sea Surface Salinity (SSS) variability from a hindcast run of an oceanic general circulation model (OGCM) forced by daily NCEP-NCAR reanalysis from 1990 to 2001 is analyzed. The purpose is to test the capability of the model in terms of the salinity simulation and provide insights for the future SSS observation from space. With daily forcing, the model can reproduce SSS change of the tropical Pacific on different time scales by comparing with the Tropical Atmosphere Ocean (TAO) mooring observation. Our model results show that the western tropical Pacific is a large variability center on different time scales. On the interannual time scale, the standard deviation of SSS in the region could reach 0.5 practical salinity unit (psu). However, the eastern tropical Pacific shows relatively weak SSS variability (0.1 psu). On the intraannual time scale (60–360 days), the SSS variability in the western tropical Pacific is around 0.2 psu. The model SSS variability for the intraseasonal time scale (30–60 days) has a magnitude around 0.1 psu and tends to elongate along the latitudes of large meridional SSS gradient. On time scale shorter than 30 days, the model SSS variability center is near the equator and has a magnitude less than 0.1 psu. Relevance to the upcoming salinity satellite mission is discussed. *INDEX TERMS:* 4215 Oceanography: General: Climate and interannual variability (3309); 4251 Oceanography: General: Marine pollution; 4271 Oceanography: General: Physical and chemical properties of seawater; 4227 Oceanography: General: Diurnal, seasonal, and annual cycles; 4522 Oceanography: Physical: El Nino. **Citation:** Wang, X., and Y. Chao (2004), Simulated Sea Surface Salinity variability in the tropical Pacific, *Geophys. Res. Lett.*, *31*, L02302, doi:10.1029/2003GL018146.

1. Introduction

[2] The spatial and temporal variability of ocean salinity is poorly known mostly because of the sparse *in situ* observation. The effects of salinity on oceanic dynamics, however, are widely recognized. Motivated by the upcoming salinity satellite mission, the SSS variability simulated by an OGCM is analyzed in the present research. Previous attempts to describe the seasonal and interannual SSS variability in the tropical Pacific [e.g., *Delcroix*, 1998] made use of the available observations and provided valuable information. However, the salinity observation is very sparse in space, and this leaves unresolved many aspects of SSS variability on different time scales. The goal of the salinity satellite programs is to provide higher resolution surface data which can be analyzed and blended with *in situ* observations and OGCMs to gain a more comprehensive dynamical understanding. This study is a first step toward this long-term goal by analyzing an OGCM simulation and comparing the available SSS observations. With an OGCM, we estimate the SSS variability on different time scales, including the interannual (time scale longer than 360 days), intraannual (60–360 days), intraseasonal (30–60 days), and the time scale shorter than 30 days that might be aliased, since the proposed satellite SSS observation has a temporal resolution of one month. Based on the simulated SSS variability, we assess what dynamically important salinity signals the future salinity satellite mission can resolve.

[3] Forced by 1990–2001 daily air-sea fluxes derived from the NCEP-NCAR (National Centers for Environmental Prediction, National Center for Atmospheric Research) reanalysis [*Kalnay et al.*, 1996], our OGCM hindcast can generally reproduce the SSS change on different time scales in the tropical Pacific. The 5-day averaged model output is first compared with TAO mooring observation [*McPhaden et al.*, 1998] site by site. All the available mooring salinity data at each site in upper 10 m is averaged to form a 5-day averaged SSS for that mooring site for comparison. Then the 360-day low-pass filtered, 60–360-day and 30–60-day band-pass filtered and 30-day high-pass filtered model SSS are used to analyze its variability. The model and forcing fields are discussed in section 2. In section 3, we compare the model result with observations. Section 4 discusses the mean seasonal cycle of model SSS and its variability. Section 5 summarizes our results and its implications to the future salinity satellite missions.

2. Model and Forcing Fields

[4] The OGCM used is based on a terrain-following vertical coordinate primitive equation model, known as the Regional Oceanic Modeling System [*Shchepetkin and McWilliams*, 2003]. The model has a horizontal resolution of 50 km in both zonal and meridional direction and 20 levels in vertical direction. The model covers the Pacific region from 45°S to 65°N and from 99°E to 70°W with realistic coastline and bathymetry. An open boundary condition [*Marchesiello et al.*, 2001] is used along its western boundary. The KPP scheme [*Large et al.*, 1994] is used for vertical viscosity and diffusivity. The model is first integrated for 60 years with climatological air-sea fluxes from the Comprehensive Ocean-Atmosphere Data Set [*da Silva et al.*, 1994]. After 60 years integration the model reached a quasi-steady state. The model climatological state is comparable to the observation and results from other OGCMs with similar horizontal and vertical resolution.

[5] Starting from the model climatological state after the 60 year integration, the model is integrated further with monthly NCEP-NCAR reanalysis from 1948 to 1989 and daily reanalysis from 1990 to 2001. The 5-day averaged model output from 1990 to 2001 is used in the present research. The details of the forcing field derivation are

0094-8276/04/2003GL018146$05.00

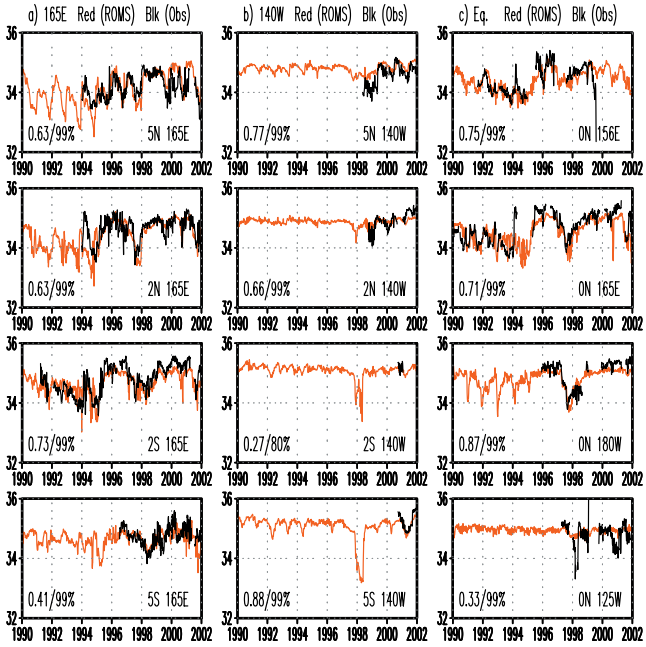

Figure 1. The comparison of 5-day averaged model sea surface salinity and Tropical Atmosphere Ocean mooring observation along 165°E (left), 140°W (middle), and the Equator (right). The red line is for model output. The black line is for observation. The correlation coefficient and its significance level are listed in the lower left corner of each figure. The unit for salinity is psu.

similar to that in *Li et al.* [2001]. In the experiment, no restoring terms are used for sea surface temperature (SST) and SSS. Our study is similar to *Doney et al.* [2003] in the sense that the model is integrated in a hindcast mode. In terms of fresh water flux forcing, *Doney et al.* [2003] recognized the excessive precipitation of the *Xie and Arkin* [1996] data set in the tropical Pacific (110°–230°E, 16°S–15°N) and replaced *Xie and Arkin* [1996] values with satellite precipitation estimates. Our comparison of the NCEP-NCAR reanalysis precipitation and *Xie and Arkin* [1996] data set shows that these two data sets have similar spatial structure and time evolution in interannual precipitation variability, however the magnitude of precipitation variability in *Xie and Arkin* [1996] is twice as large as that of the NCEP-NCAR precipitation (figures not shown).

3. Comparison With Observation

[6] The 5-day averaged model SSS compares well with the TAO observation, especially in the western tropical Pacific (Figure 1). The model can reproduce the interannual variability during this period, especially the 1997–1998 ENSO event. In terms of salinity, the ENSO event shows up as a freshening of the whole equatorial Pacific in 1997 and 1998. The freshening in the western equatorial Pacific occurs in 1997. In the eastern equatorial Pacific, the freshening occurs toward the end of 1997 or early 1998 in the model. The model can also reproduce the salinity change on the intraannual time scale. On the intraseasonal time scale, the magnitude of salinity variability from the model is comparable with that of the observation, although we are not expecting a close match for the phase of SSS evolution. The averaged correlation coefficient between the model output and observation from all 12 sites is 0.63. The correlation coefficients are significant at a level of 99% for all the comparing sites except at 2°S–140°W which has a very short observation (25 5-day periods). Even at this site, the model SSS and observation are of the same magnitude. Our model simulation is also verified using SST observation (figure ignored). On interannual time scale, the warm events in 1991–1992, 1993, 1994, and 1997–1998 are reproduced, and so are the cold events in 1995–1996, 1998–1999 and 1999–2000.

4. Simulated SSS Variability

[7] The annual mean SSS from the model (Figure 2a) compares favorably with the observation [e.g., Figure 2b in *Delcroix* [1998]]. The northern tropical Pacific along 10°N is a region of relatively fresh water with salinity less than 34.8 psu, which is roughly under the Intertropical Convergence Zone. Both the northern and the southern sides of the fresh water band are regions of large meridional SSS gradient. Between the fresh water in the western tropical Pacific and the salty water to the east, there is a region of large salinity gradient in the longitude band of 160°E to 180°E. In the southwestern tropical Pacific, there is also a region of relatively fresh water under the South Pacific Convergence Zone. The southeastern tropical Pacific is a region of high salinity (higher than 36 psu). Thus, there is a region of large salinity gradient along 160°W in the southern tropical Pacific. Similar to the situation in the northwestern tropical Pacific, there is a region of large meridional salinity gradient along 20°–25°S. These large salinity gradient regions tend to have large SSS variability on different time scales.

[8] The mean seasonal cycle of the 5-day averaged model output is consistent with previous studies in terms of spatial pattern and magnitude [*Delcroix*, 1998]. Compared with the results of *Delcroix* [1998] which made use of sparse data with monthly interpolations, the model results here show detailed structures from 30°S to 30°N since 5-day averaged output is used and has a full spatial coverage. The major features are discussed briefly to provide the background for later discussion. There are three regions that have a strong seasonal cycle (Figure 2b): northwestern tropical Pacific (5°N–15°N, 140°E–180°E), northeastern tropical Pacific (5°N–15°N, 140°W–80°W), and southwestern tropical Pacific (10°S–20°S, 160°E–160°W). These three regions are associated with relatively fresh water (Figure 2a) and large annual precipitation (figure ignored). Consistent with *Delcroix* [1998], the model mean seasonal cycle of SSS in the tropical Pacific is closely related with that of the precipitation. The maximum precipitation leads the minimum salinity by three months.

[9] After removing the mean seasonal cycle, the model SSS is 360-day low-pass filtered, 60–360-day band-pass filtered, 30–60-day band-pass filtered, and 30-day high-pass filtered to analyze the SSS variability on interannual, intraannual and intraseasonal time scales, respectively. The western tropical Pacific is a SSS variability center on the interannual, intraannual and intraseasonal time scales (Figure 3). The centers of strong mean seasonal cycle are

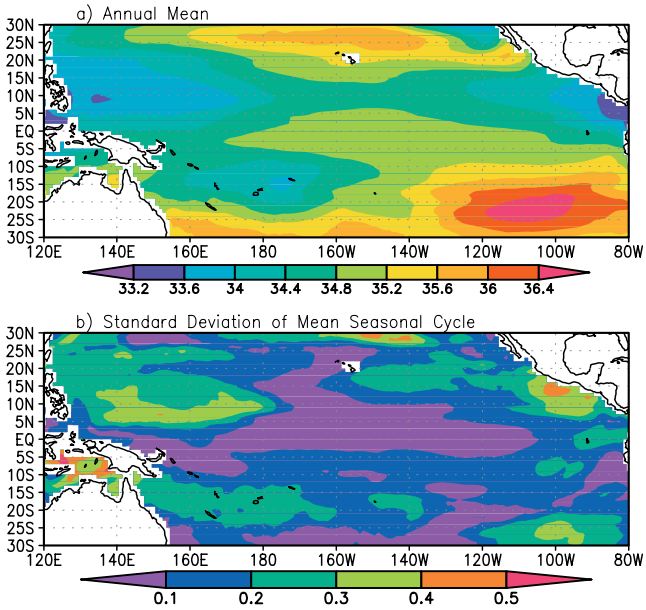

Figure 2. The annual mean SSS (a) and the standard deviation (b) of mean seasonal cycle using the 5-day averaged model output from 1990 to 2001. Unit is psu. Note the colorbar is different in (a) and (b).

associated with fresh water and large annual precipitation. However, the model SSS variability centers on interannual, intraannual and intraseasonal time scales tend to be located in regions of large salinity gradient. On the interannual time scale, there are two centers with a magnitude around 0.5 psu embedded in the large variability region of the western tropical Pacific. One is located around 0°–10°N, 150°E–170°E. The other is located around 15°–25°S and extends from 160°E to 140°W. These two centers are associated with large zonal and/or meridional salinity gradient (Figure 2a). In contrast to the western tropical Pacific, the eastern tropical Pacific has a relatively weak SSS variability (0.1 psu).

[10] On the intraannual time scale (Figure 3b), the regions that have large SSS variability are the northwestern, southwestern, and the northeastern tropical Pacific along the central America coast. The standard deviation associated with this time scale is around 0.2 psu. These regions are the regions of strong mean seasonal cycle combined with regions of large SSS gradient (Figure 2). Our analysis shows that the model SSS variability on this time scale tends to propagate westward along 15°N and 15°S with a phase speed around 0.1–0.2 m/s and a spatial scale of 20–40 degrees. While the model SSS variability in the western equatorial Pacific does not show much propagation and even propagates eastward. The nature of this SSS variability is not yet understood. It is interesting to note here that the mean current also has strong shear along 15°–20°N(S) belts (figure ignored). The location of model SSS variability centers on the intraseasonal time scale (Figure 3c) is similar to that on the intraannual time scale, except that the magnitude is reduced to around 0.1 psu. The variability centers on this time scale tend to elongate along certain latitudes, such as 22°N, 15°N, 5°N, the equator, 5°S, 15°S. Except the centers along 15°N and 15°S which extend to the eastern Pacific, other centers extend to around the dateline. This leaves the northeastern and southeastern tropical Pacific a region of small variability. The large variability centers along 15°N and 15°S, especially east of 160°W, are associated with large meridional SSS gradient. This implies that on intraseasonal time scale the anomalous meridional advection of mean SSS plays a role for model SSS variability. On the time scale shorter than 30 days, though the variability centers of the intraseasonal time scale along 15°N and 15°S are still visible, the major variability center is along the equator with a magnitude around 0.06 psu.

5. Conclusion and Discussion

[11] The capability of an OGCM in simulating SSS is first evaluated against the available observations. The simulated SSS is then used to quantify the mean seasonal cycle of SSS and its variability on different time scales including the interannual, intraannual and intraseasonal. The regions that have a strong mean seasonal cycle in the tropical

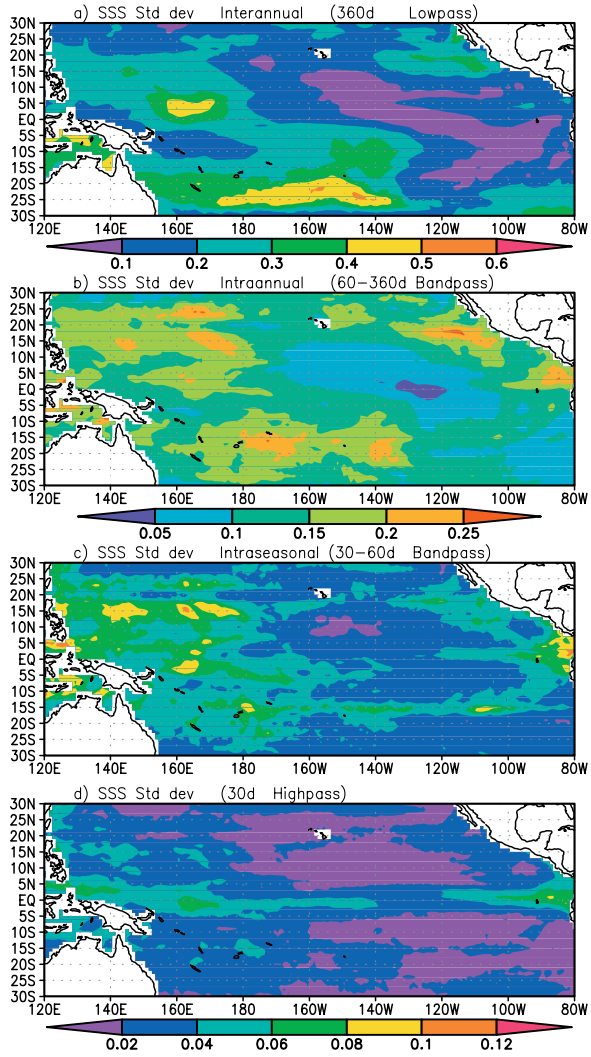

Figure 3. The standard deviation of 5-day averaged model SSS for 1990–2001: (a) 360-day low-pass filtered; (b) 60–360 day band-pass filtered; (c) 30–60 day band-pass filtered; (d) 30-day high-pass filtered. Unit is psu. Note the colorbar for (c) and (d) is the same, and different from those in (a) and (b) respectively.

Pacific are associated with relatively fresh water and large annual precipitation.

[12] The western tropical Pacific is a region of large variability on interannual, intraannual, and intraseasonal time scales. The subtle and visible difference of the spatial distribution of model SSS variability indicates that different mechanisms are responsible for the SSS variability on different time scales. On the interannual time scale, the western tropical Pacific has a standard deviation as high as 0.5 psu. On the intraannual time scale (60–360 days), centers of model SSS variability tend to be regions of strong mean seasonal cycle combined with regions of large salinity gradient. The magnitude of model SSS variability on this time scale is around 0.2 psu. On the intraseasonal time scale (30–60 days) the spatial distribution of model SSS variability bears similarity to that on the intraannual time scale but with a standard deviation around 0.1 psu. The variability centers on this time scale tend to elongate along certain latitudes that have large meridional SSS gradient. The results from this type hindcast integration are unavoidably influenced by the accuracy of the model and the forcing fields. For SSS variability in particular, the uncertainty of precipitation estimation is a concern. To fully address the issue of SSS variability, an optimal estimate of the ocean state by combining model and observation is needed.

[13] The results reported here confirm the designing strategy of the upcoming SSS satellite mission. For example, with an anticipated accuracy of 0.2 psu for monthly averaged salinity and a mission life of 3 years, satellite salinity observation will be able to detect the intraannual to interannual salinity changes. Our modeling estimates of the SSS variability shorter than 30 days also suggest that the aliasing error of SSS fluctuations to the monthly averaged map should be less than 0.1 psu, significantly smaller than the science requirements of 0.2 psu. Our modeling ability to simulate SSS will be continuously improved in the coming years in anticipation of interpreting and assimilating the SSS observation.

[14] **Acknowledgments.** The research was carried out by the Jet Propulsion Laboratory (JPL), California Institute of Technology, under contract with National Aeronautics and Space Administration. Computations were performed on the SGI Origin 3000 computers at JPL and NASA Ames Research Center. We acknowledge the support from the JPL Supercomputing Project. Discussions with Jim McWilliams, Patrick Marchesiello, Alexander Shchepetkin about the use of ROMS and with Michael J. McPhaden about salinity variability are acknowledged. Comments from Gary Lagerloef and another anonymous reviewer helped us in improving the original manuscript. Tony Song and Yury N. Golubev provided technical help in setting up the ocean model.

References

da Silva, A. M., C. C. Young, and S. Levitus (1994), Atlas of Surface Marine Data 1994, Vol. 1, NOAA Atlas NESDIS, 83pp.

Delcroix, T. (1998), Observed surface oceanic and atmospheric variability in the tropical Pacific at seasonal and ENSO timescales: A tentative overview, *J. Geophys. Res.*, *103*(C9), 18,611–18,633.

Doney, S. C., S. Yeager, G. Danabasoglu, W. G. Large, and J. C. McWilliams (2003), Simulating global oceanic interannual variability using historical climate forcing (1958–1997), *J. Climate*, (in press).

Kalnay, E., et al. (1996), The NCEP/NCAR 40-year reanalysis project, *Bull. Amer. Meteor. Soc.*, *77*, 437–471.

Large, W. G., J. C. McWilliams, and S. C. Doney (1994), Oceanic vertical mixing: a review and a model with nonlocal boundary layer parameterization, *Rev. Geophys.*, *32*, 363–403.

Li, X., Y. Chao, J. C. McWilliams, and L.-L. Fu (2001), A comparison of two vertical-mixing schemes in a Pacific ocean general circulation model, *Climate, J.*, *14*, 1377–1398.

Marchesiello, P., J. C. McWilliams, and A. Shchepetkin (2001), Open boundary conditions for long-term integration of regional oceanic models, *Ocean Modelling*, *3*, 1–20.

McPhaden, M. J., et al. (1998), The Tropical Ocean Global Atmosphere (TOGA) observing system: A decade of progress, *J. Geophys. Res.*, *103*, 14,169–14,240.

Shchepetkin, A. F., and J. C. McWilliams (2003), The Regional Oceanic Modeling System: A split-explicit, free-surface, topography-following-coordinate ocean model, *Ocean Modelling*, submitted.

Xie, P., and P. A. Arkin (1996), Analysis of global monthly precipitation using gauge observations, satellite estimates, and numerical model predictions, *J. Climate*, *9*, 840–858.

Y. Chao and X. Wang, M/S 300-323 Jet Propulsion Laboratory, California Institute of Technology, 4800 Oak Grove Drive, Pasadena, CA 91109, USA. (yi.chao@jpl.nasa.gov; xiao@pacific.jpl.nasa.gov)